Hindawi Publishing Corporation
EURASIP Journal on Wireless Communications and Networking
Volume 2008, Article ID 541478, 8 pages
doi:10.1155/2008/541478

*Research Article*

# Design and Performance of Cyclic Delay Diversity in UWB-OFDM Systems

**Poramate Tarasak, Khiam-Boon Png, Xiaoming Peng, and Francois Chin**

*Institute for Infocomm Research, 21 Heng Mui Keng Terrace, Singapore 119613*

Correspondence should be addressed to Poramate Tarasak, ptarasak@i2r.a-star.edu.sg

Received 14 June 2007; Revised 20 October 2007; Accepted 9 December 2007

Recommended by Stefan Kaiser

This paper addresses cyclic delay diversity (CDD) in an ultra-wideband communication system based on orthogonal frequency division multiplexing (OFDM) technique. Symbol error rate and outage probability have been derived. It is shown that with only two transmit antennas, CDD effectively improves SER performance and reduces outage probability significantly especially when the channel delay spread is short. Both simulation and analytical results agree well in all considered cases. The selection of delay times for CDD is also addressed for some special cases.



## 1. INTRODUCTION

Wireless personal area network (WPAN) using ultra-wideband (UWB) communication has received great interest due to its capability of transmitting very high bit rate over short range. Conventional UWB technique transmits very short pulses in a time-hopping manner with low-duty cycle [1]. In addition to high bit rate transmission, due to its short-pulse structure, UWB also has high precision localization capability. However, pulse-based UWB system can be very difficult to implement since it requires analog-to-digital and digital-to-analog converters with very high sampling rate when very high-transmission rate is needed. Alternate UWB technique, so-called multiband OFDM (MB-OFDM), was proposed to divide the wide bandwidth into smaller bands. The OFDM symbols are transmitted across the bands according to time-frequency code [2]. MB-OFDM has been adopted in the WiMedia standard as a transmission technique for UWB systems becoming ISO standard [3]. This latter technique will be considered in this paper.

To enhance system performance, multiple antennas could be applied with the UWB system to obtain spatial diversity. However, multiple-antenna technique typically incurs higher complexity at both transmitter and receiver. Cyclic delay diversity (CDD), which is a low-complexity diversity scheme for OFDM systems [4, 5], is more suitable for UWB system. Although CDD can be applied equivalently at either transmitter or receiver, this paper will only focus on CDD at the transmitter. CDD adds a deterministic delay to the effective part of the OFDM symbol after IFFT processing at each transmit antenna. The time delay results in phase rotation in the frequency domain among the subcarriers. By choosing appropriate delay times, the CDD scheme is able to achieve a reduced correlation of the effective frequency response. That means CDD yields higher-frequency selectivity and then the error performance is improved when coding is applied across subcarriers. Effectively, CDD converts spatial diversity associated with multiple transmit antennas into frequency diversity in the equivalent single antenna system. This technique is elegant and beneficial because diversity gain can be achieved without modification at the receiver (or at the transmitter in the case of CDD applied at the receiver). Therefore, it has received considerable attention in the system design where backward compatibility is an important issue. In addition, compared to space-frequency coding technique, CDD requires only one IFFT processor at the transmitter regardless of the number of transmit antennas while space-frequency coding requires the number of IFFT processors equal to the number of transmit antennas. Recently, the impact of channel fading correlation on the performance of CDD has been investigated in [6].

Research on UWB with MB-OFDM technique is relatively new compared to that with pulse-based technique. Recent efforts to improve the system performance include using

advanced coding or multiple antennas. Low-density parity-check code (LDPC code) for MB-OFDM has been evaluated in [7] and a simplified LDPC has also been proposed to achieve low complexity without sacrificing performance. Reference [8] evaluates the performance of space-time block code (STBC) and convolutional STBC (CC-STBC) on a series of channel models at different rates and concludes that CC-STBC can be considered for extreme channel environment. Reference [9] investigates concatenated Reed-Solomon and convolutional codes and shows that it outperforms the convolutional code at high SNR. More recently, MIMO technique and cooperative communication have been applied to UWB system, for example, [10, 11]. Notably, [11] applies decode-and-forward protocol to improve communication range and reduce power consumption.

This paper exploits CDD which aims to improve the performance of UWB-OFDM system with low complexity. We adopt the channel model similar to [12] which includes the effects of multipath clustering and Poisson arrival of multipath components inherited in UWB channels. Based on the framework in [12], symbol error rate (SER) and outage probability have been derived for the CDD case. Some complication in the evaluation of outage probability that was not found in [12] is also addressed. Simulation and analytical results show that CDD improves the SER performance and reduces outage probability significantly due to its diversity advantage. The results clearly indicate the performance depending on channel environment and number of coded symbols across subcarriers. Since delay time selection has significant influence to the performance, the optimum delay times to minimize SER are proposed which minimize the determinant of the correlation matrix of the effective channel. It is also shown that the selection approach in [4] is optimum when the number of transmit antennas is equal to the number of coded symbols across subcarriers at high $E_b/N_0$ region.

The paper is organized as follows. Section 2 presents system and channel models. Section 3 discusses the application of CDD. Section 4 derives the SER and outage probability. Section 5 shows simulation results and draws some discussions. Section 6 addresses the issue of delay time selection. Conclusion is given in Section 7. The notations in this paper will closely follow those in [12] for consistency.

## 2. SYSTEM MODEL

We consider a point-to-point communication system using UWB-OFDM system. Although this paper considers a single-band approach, multiband OFDM can be readily extended [12]. The following briefly explains the channel model and signal model taken from [12].

### 2.1. Channel model

The channel model in [12] is based on the Saleh-Valenzuela (S-V) model for indoor environment. Let $h(t)$ be an impulse response which can be written as

$$h(t) = \sum_{c=0}^{C} \sum_{l=0}^{L} \alpha(c,l)\delta(t - T_c - \tau_{c,l}), \tag{1}$$

where $\alpha(c,l)$ is the $l$th multipath component of the $c$th cluster, $T_c$ is the delay of the $c$th cluster, and $\tau_{c,l}$ is the delay of $\alpha(c,l)$ relative to $T_c$. According to (1), the total number of clusters is $C+1$ and the total number of channel taps is $L+1$. Both cluster arrival and multipath arrival follow Poisson distribution with rate $\Lambda$ and $\lambda$, respectively. Note that it is possible for clusters to be overlapped. $\alpha(c,l)$ are zero-mean complex Gaussian random variables whose variances are

$$\Omega_{c,l} = E\left[\,|\alpha(c,l)|^2\right] = \Omega_{0,0}e^{-T_c/\Gamma - \tau_{c,l}/\gamma}, \tag{2}$$

where $\Omega_{0,0}$ is the mean energy of the first path of the first cluster, $\Gamma$ and $\gamma$ are power decay factors for cluster and multipath, respectively. $E[\cdot]$ is an expectation. For a fair comparison, total multipath energy is normalized to one, that is, $\sum_{c=0}^{C}\sum_{l=0}^{L}\Omega_{c,l} = 1$.

Comparing with the standard channel model in IEEE802.15.3a [13], two main differences are observed. First, $\alpha(c,l)$ is Gaussian distributed as opposed to log-normal distributed. Second, the log-normal shadowing effect has been neglected. Nevertheless, the potential advantage of CDD should be valid on a more realistic channel model as well.

### 2.2. Signal model

Assuming perfect synchronization and channel estimation at the receiver, the received signal at $n$th subcarriers, $n = 0, 1, \ldots, N-1$, after removing cyclic prefix and performing FFT is

$$y(n) = \sqrt{E_s}d(n)H(n) + z(n), \tag{3}$$

where $E_s$ is the symbol energy, $d(n)$ is a transmitted symbol. $z(n)$ is a zero-mean complex Gaussian noise with variance $N_0$ . $H(n)$ is the channel transfer function at the $n$th subcarrier obtained from

$$H(n) = \sum_{c=0}^{C} \sum_{l=0}^{L} \alpha(c,l)\exp\left(-j2\pi n\Delta f\left(T_c + \tau_{c,l}\right)\right), \tag{4}$$

where $j = \sqrt{-1}$, $\Delta f$ is the subcarrier spacing. The above signal model corresponds to conventional UWB-OFDM system. The signal model for CDD will be described in the next section.

In this paper, we are considering the coded system with and without CDD. The code used is a repetition code based on a symbol level which is achieved by repeating the symbols on adjacent subcarriers. The symbols are repeated $M$ times in the case of coding across $M$ subcarriers resulting in code rate $1/M$ . Figure 1 shows the block diagrams of a transmitter with/without CDD and a receiver considered in this paper.

## 3. CYCLIC DELAY DIVERSITY

We are considering the system with $N_t$ transmit antennas and single receive antenna. At the transmitter, CDD makes $N_t$ copies of a transmit stream after IFFT processing of a coded symbol stream, where $N_t$ is the number of transmit antennas. At each antenna, each copy of the OFDM symbol is cyclically delayed by $\delta_{n_t}$, that is, part of the symbol that has been

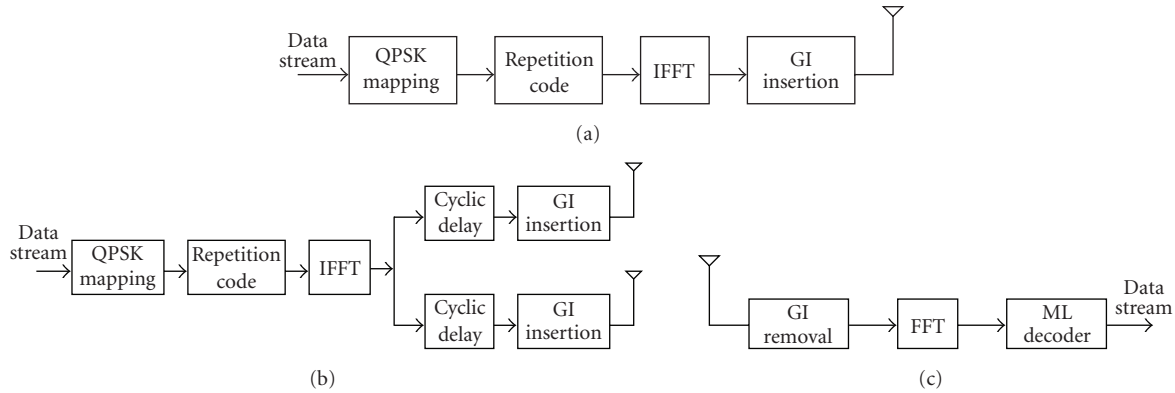


Figure 1: (a) A transmitter without CDD. (b) A transmitter with CDD (two transmit antennas). (c) A receiver for UWB-OFDM system.

delayed beyond an OFDM symbol period is added at the beginning [4]. Then cyclic prefix of length longer than the delay spread (guard interval) is added at each antenna. All streams are transmitted simultaneously.

Since cyclic delay is done on the time-domain signal, it corresponds to phase rotation in the frequency domain. At the receiver, the channel transfer function appears to be a superposition of channel transfer functions from all transmit antennas with the corresponding phase shifts [4],

$$H_{\text{eff}}(n) = \sum_{n_t=0}^{N_t-1} H_{n_t}(n)\exp\left(-j\frac{2\pi\delta_{n_t}n}{N}\right), \tag{5}$$

where $H_{\text{eff}}(n)$ denotes the effective channel, $H_{n_t}(n)$ denotes the channel transfer function from the $n_t$th antenna. For a fair comparison, the transmitted symbol energy must be scaled by $1/\sqrt{N_t}$ so the total signal energy remains unchanged compared to a single-antenna system. It can be readily seen from (5) that $H_{\text{eff}}(n)$ has higher fluctuation and therefore a higher amount of frequency diversity when coding is applied across the subcarriers.

Selection of $\{\delta_{n_t}\}$ is an important issue that affects the performance of CDD. Witrisal et al. [4] proposed selection of delays from

$$\delta_{n_t} = n_t \cdot \frac{N}{N_t}, \tag{6}$$

assuming $N_t$ divides $N$. This choice yields largest delay differences and zero correlation between adjacent $N_t$ subcarriers [4]. This choice of delay times will be further justified in Section 6.

Regarding coding to be used, [14] comments on the minimum $N_t$ which must be $N_t \le d_f$, where $d_f$ is the minimum distance of the coded symbols. With a repetition code rate $1/M$, this condition becomes $N_t \le M$, otherwise, CDD cannot achieve full-diversity advantage. Therefore, we will consider only the case where this condition is satisfied.

## 4. SYMBOL ERROR RATE AND OUTAGE PROBABILITY ANALYSIS

In this section, we derive pairwise error probability (PEP) and outage probability for the CDD cases.

### 4.1. Pairwise error probability

PEP in this section is the probability of decoding to an error symbol $\hat{d}(n)$ instead of the transmitted symbol $d(n)$ . Let the Euclidean distance between these two symbols be $\nu_n$. The received signal is rewritten in a matrix form as

$$\mathbf{Y} = \sqrt{E_s/N_t}X(\mathbf{D})\mathbf{H}^{\text{eff}} + \mathbf{Z}, \tag{7}$$

where $\mathbf{Y} = [y(0) \quad y(1) \quad \cdots \quad y(M-1)]^t$, $(\cdot)^t$ is a transpose operation, $X(\mathbf{D}) = \text{diag}(d(0), d(1), \ldots, d(M-1))$ is an $M \times M$ diagonal matrix with the $[d(0), d(1), \ldots, d(M-1)]$ as its main diagonal. The $M \times 1$ channel vector $\mathbf{H}^{\text{eff}}$ represents the effective channel transfer function which is $[H_{\text{eff}}(0), H_{\text{eff}}(1), \ldots, H_{\text{eff}}(M-1)]^t$ corresponding to $M$ symbol intervals. The $M \times 1$ vector $\mathbf{Z} = [z(0) \quad z(1) \quad \cdots \quad z(M-1)]^t$ is a noise vector. With maximum likelihood decoder, the decision rule is

$$\hat{\mathbf{D}} = \arg\min_{\mathbf{D}} \left\| \mathbf{Y} - \sqrt{E_s/N_t}X(\mathbf{D})\mathbf{H}^{\text{eff}} \right\|^2, \tag{8}$$

where $\|\cdot\|$ denotes the Frobenius norm.

Follow the same line of derivation in [12], let us define a correlation matrix of the effective channel, $\mathbf{R}_M^{\text{eff}} = E[\mathbf{H}^{\text{eff}}\mathbf{H}^{\text{eff}^{\mathcal{H}}}]$. $(\cdot)^{\mathcal{H}}$ is a conjugate transpose operation. The PEP of CDD of a UWB-OFDM system is readily obtained as [12, Theorem 2]

$$P_e \approx \frac{1}{\pi}\int_0^{\pi/2}\prod_{n=1}^{M}\left(1 + \frac{\rho\nu_n}{4N_t\sin^2\theta}\text{eig}_n(\mathbf{R}_M^{\text{eff}})\right)^{-1} d\theta, \tag{9}$$

where $\rho = E_s/N_0$, $\text{eig}_n(\mathbf{R}_M^{\text{eff}})$ is $n$th eigenvalue of the matrix $\mathbf{R}_M^{\text{eff}}$. The integration over the variable $\theta$ comes from using an alternate representation of $Q$ function [12].

To find $\mathbf{R}_M^{\text{eff}}, \mathbf{H}^{\text{eff}}$ is written as

$$\mathbf{H}^{\text{eff}} = \Xi\mathbf{H}, \tag{10}$$

where $\mathbf{H} = [H_0(0), H_1(0), \ldots, H_{N_t-1}(0), \ldots, H_0(M-1), H_1(M-1), \ldots, H_{N_t-1}(M-1)]^t$. $\Xi$ is an $M \times N_t M$ phase matrix written as

$$\Xi = \begin{bmatrix} \phi(0) & \mathbf{0}_{1\times N_t} & \cdots & \mathbf{0}_{1\times N_t} \\ \mathbf{0}_{1\times N_t} & \phi(1) & \cdots & \mathbf{0}_{1\times N_t} \\ \vdots & \vdots & \ddots & \vdots \\ \mathbf{0}_{1\times N_t} & \mathbf{0}_{1\times N_t} & \cdots & \phi(M-1) \end{bmatrix}, \tag{11}$$

where $\phi(n)$ is a $1 \times N_t$ phase vector, $\phi(n) = [\exp(-j(2\pi\delta_0 n/N)), \exp(-j(2\pi\delta_1 n/N)), \ldots, \exp(-j(2\pi\delta_{N_t-1} n/N))]$, $\mathbf{0}_{1\times N_t}$ is a $1 \times N_t$ all-zero vector. Therefore, the correlation matrix $\mathbf{R}_M^{\text{eff}}$ is found from

$$\begin{aligned} \mathbf{R}_M^{\text{eff}} &= E[\mathbf{H}^{\text{eff}}\mathbf{H}^{\text{eff}^{\mathcal{H}}}] = E[\Xi\,\mathbf{H}\mathbf{H}^{\mathcal{H}}\Xi^{\mathcal{H}}] \\ &= \Xi E[\mathbf{H}\mathbf{H}^{\mathcal{H}}]\Xi^{\mathcal{H}} = \Xi(\mathbf{R}_M \otimes \mathbf{I}_{N_t})\Xi^{\mathcal{H}}, \end{aligned} \tag{12}$$

where $\mathbf{I}_{N_t}$ is an $N_t \times N_t$ identity matrix, $\otimes$ is a Kronecker product and

$$\mathbf{R}_M = \begin{bmatrix} 1 & R(1)^* & \cdots & R(M-1)^* \\ R(1) & 1 & \cdots & R(M-2)^* \\ \vdots & \vdots & \ddots & \vdots \\ R(M-1) & R(M-2) & \cdots & 1 \end{bmatrix}, \tag{13}$$

which corresponds to the correlation matrix of the channel transfer function in the single antenna case. Each element $R(m)$ can be found from [12]

$$R(m) = \Omega_{0,0} \cdot \frac{\Lambda + g(1/\Gamma, m)}{g(1/\Gamma, m)} \cdot \frac{\lambda + g(1/\gamma, m)}{g(1/\gamma, m)}, \tag{14}$$

where $g(a, m) = a + j2\pi m\Delta f$. From the PEP, SER can be computed using a well-known union bound, that is, by summing the PEP corresponding to each incorrect symbol.

### 4.2. Outage probability

Outage probability for CDD case is defined as the probability that the combined effective SNR falls below a specified threshold $\zeta_0$. The combined SNR in this case is

$$\zeta = \frac{\rho}{N_t M} \sum_{n=0}^{M-1} |H^{\text{eff}}(n)|^2, \tag{15}$$

where $\rho = E_s/N_0$ is the SNR per transmitted symbol. Therefore, the outage probability can be expressed as

$$\begin{aligned} P_{\text{out}} &= P(\zeta \le \zeta_0) = P\left(\xi_{\text{eff}} \le \frac{MN_t\zeta_0}{\rho}\right) \\ &= \int_0^{(MN_t\zeta_0/\rho)} p_{\xi_{\text{eff}}}(x)dx, \end{aligned} \tag{16}$$

where $\xi_{\text{eff}} = \sum_{n=0}^{M-1} |H^{\text{eff}}(n)|^2$ and $p_{\xi_{\text{eff}}}(x)$ is the probability density function of $\xi_{\text{eff}}$. Following the approach in [12], we have to find the moment-generating function (MGF) and do inverse Laplace transform in order to obtain $p_{\xi_{\text{eff}}}(x)$ and then find $P_{\text{out}}$. Having done so, we may arrive at the MGF and outage probability, respectively, as [12]

$$\mathcal{M}_{\xi_{\text{eff}}}(s) = \prod_{n=1}^{M} \frac{1}{1 - s\text{eig}_n(\mathbf{R}_M^{\text{eff}})} = \sum_{n=1}^{M} \frac{A_n}{1 - s\text{eig}_n(\mathbf{R}_M^{\text{eff}})}, \tag{17}$$

$$P_{\text{out}} = \sum_{n=1}^{M} A_n \left(1 - \exp\left(-\frac{\zeta_0 MN_t}{\rho\text{eig}_n(\mathbf{R}_M^{\text{eff}})}\right)\right), \tag{18}$$

where

$$A_n = \prod_{n'=1, n'\neq n}^{M} \frac{\text{eig}_n(\mathbf{R}_M^{\text{eff}})}{\text{eig}_n(\mathbf{R}_M^{\text{eff}}) - \text{eig}_{n'}(\mathbf{R}_M^{\text{eff}})}. \tag{19}$$

However, for (18) to be valid, all $\text{eig}_n(\mathbf{R}_M^{\text{eff}})$ must be distinct. This is a striking difference between CDD and the case in [12]. For CDD case, we have to do it is possible that some eigenvalues will be the same and repeated roots will appear in the denominator of (17). In such cases, partial fraction and higher-order inverse Laplace transform according to the obtained eigenvalues case by case.

For example, in the case of 128-point FFT, two transmit antennas and coding across four subcarriers, that is, $N = 128$, $N_t = 2$, $M = 4$, $\delta_0 = 0$, $\delta_1 = 64$, we will have $\text{eig}_1(\mathbf{R}_4^{\text{eff}}) = \text{eig}_2(\mathbf{R}_4^{\text{eff}}) = 0.816$ and $\text{eig}_3(\mathbf{R}_4^{\text{eff}}) = \text{eig}_4(\mathbf{R}_4^{\text{eff}}) = 3.184$. The $P_{\text{out}}$ can be readily obtained as

$$\begin{aligned} P_{\text{out}} = \sum_{n=1,3} B_n^2 \Bigg[ 1 - \frac{8\zeta_0}{\rho\text{eig}_n(\mathbf{R}_4^{\text{eff}})} \exp\left(-\frac{8\zeta_0}{\rho\text{eig}_n(\mathbf{R}_4^{\text{eff}})}\right) \\ - \exp\left(-\frac{8\zeta_0}{\rho\text{eig}_n(\mathbf{R}_4^{\text{eff}})}\right) \Bigg] \\ - 2C_n \left[ 1 - \exp\left(-\frac{8\zeta_0}{\rho\text{eig}_n(\mathbf{R}_4^{\text{eff}})}\right) \right], \end{aligned} \tag{20}$$

where

$$\begin{aligned} B_1 &= \frac{\text{eig}_1(\mathbf{R}_4^{\text{eff}})}{\text{eig}_1(\mathbf{R}_4^{\text{eff}}) - \text{eig}_3(\mathbf{R}_4^{\text{eff}})}, \\ B_3 &= \frac{\text{eig}_3(\mathbf{R}_4^{\text{eff}})}{\text{eig}_3(\mathbf{R}_4^{\text{eff}}) - \text{eig}_1(\mathbf{R}_4^{\text{eff}})}, \\ C_1 &= \frac{\text{eig}_1(\mathbf{R}_4^{\text{eff}})}{\text{eig}_3(\mathbf{R}_4^{\text{eff}})} \cdot B_1^3, \qquad C_3 = \frac{\text{eig}_3(\mathbf{R}_4^{\text{eff}})}{\text{eig}_1(\mathbf{R}_4^{\text{eff}})} \cdot B_3^3. \end{aligned} \tag{21}$$

Other cases can be similarly derived with some tedious manipulations.

## 5. SIMULATION AND ANALYTICAL RESULTS

The SER and outage probability are evaluated using CM1 and CM4 channel models. CM1 and CM4 are statistical

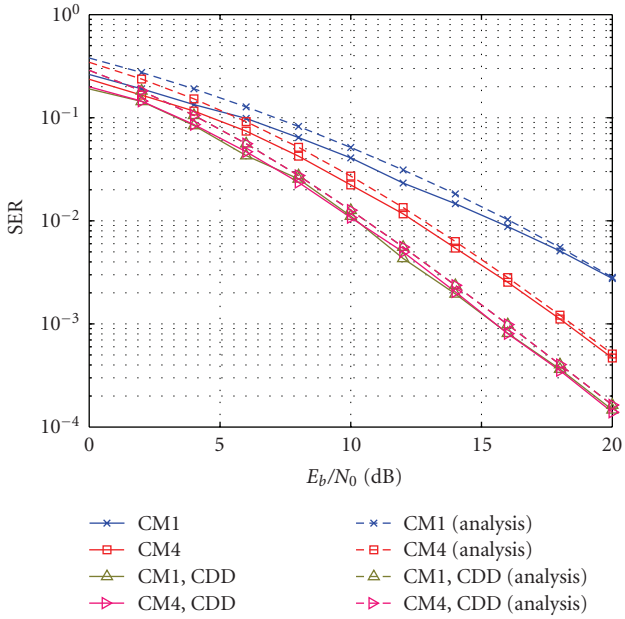


FIGURE 2: Symbol error rate of UWB-OFDM system. Jointly encoding across two subcarriers. CDD with two transmit antennas.

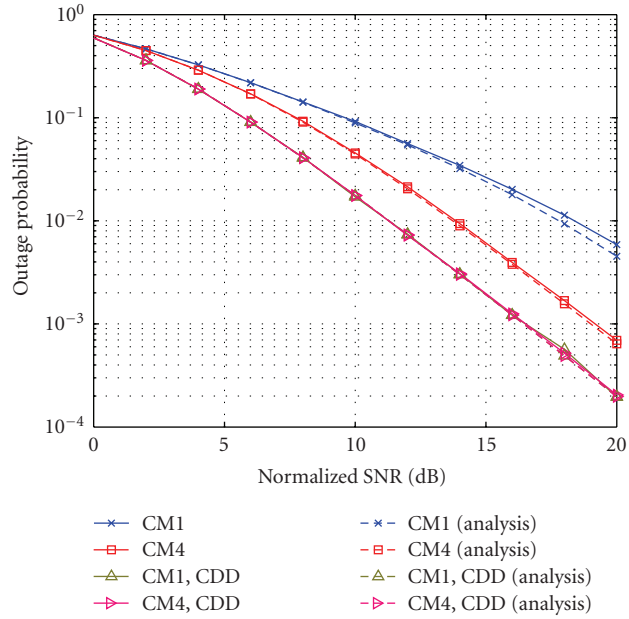


FIGURE 3: Outage probability of UWB-OFDM system. Jointly encoding across two subcarriers. CDD with two transmit antennas.

channel models whose parameters are defined to match the actual measurement data. CM1 corresponds to the indoor short range (0–4 m) line-of-sight scenario while CM4 corresponds to the indoor long-range (10 m) and extreme non-line-of-sight scenario [13]. The parameters of CM1 are $\Lambda = 0.0233 \times 10^9$, $\lambda = 2.5 \times 10^9$, $\Gamma = 7.1 \times 10^{-9}$, $\gamma = 4.3 \times 10^{-9}$; and the parameters of CM4 are $\Lambda = 0.00667 \times 10^9$, $\lambda = 2.1 \times 10^9$, $\Gamma = 24.0 \times 10^{-9}$, $\gamma = 12 \times 10^{-9}$. SER is plotted versus $E_b/N_0$ while outage probability is plotted versus the normalized SNR $= \rho/\zeta_0$. Since CM4 channel transfer function is more fluctuated than that of CM1, it gives a better performance when proper cyclic prefix is used under the condition of perfect channel estimation. (CM4 requires longer cyclic prefix than CM1 does to avoid intersymbol interference.) The UWB system has $N = 128$ subcarriers and each subband has 528 MHz bandwidth. The subcarrier spacing $\Delta f = 4.125$ MHz The data bits are mapped to QPSK symbols; and repetition code is done by repeating the symbol over $M$ subcarriers.

For CDD, we assume two transmit antennas. With the condition in (6), the delay values of $\delta_0 = 0$, $\delta_1 = 64$ are fixed in all cases. All simulation results are plotted as solid lines while analytical results are plotted as dashed lines.

Figure 2 shows SER of UWB-OFDM system with jointly encoding across two subcarriers. The performance of CDD achieves about 6 dB gain and 4 dB gain on CM1 and CM4 channels, respectively. For CDD with CM1, there is a clear improvement due to diversity advantage as seen from the steeper slopes of the curves. For CDD with CM4, the curves remain at the same slope but with an additional coding gain as shown from the horizontal shift of the curves. It is observed that with CDD, CM1, and CM4 have the same SER performance. This attributes to the fact that the delay time according to [4] causes the uncorrelated Rayleigh fading across two adjacent subcarriers regardless of the channels, which is the best case for $M = 2$ . All simulation results validate the analytical results over the whole SNR range.

Figure 3 shows the outage probability of UWB-OFDM system with jointly encoding across two subcarriers. At outage probability of $10^{-2}$, CDD obtains about 6.3 dB gain and 2.3 dB gain on the CM1 and CM4 channels, respectively. The improvement in outage probability is similar to the SER case. The slope is steeper in the CM1 case while there is a horizontal shift in the CM4 case. Both CM1 and CM4 with CDD have the same outage probability for the same reason explained for SER. Analytical results match very well to the simulation results.

Figures 4 and 5 depict the respective SER performance and outage probability for the case of jointly encoding across four subcarriers. The gaps between CM1 and CM4 performance with/without CDD become larger than those in Figure 3. At SER of $10^{-3}$, CDD achieves 6 dB gain on the CM1 channel and 2.2 dB gain on the CM4 channel. Unlike Figures 2 and 3, it is seen that there is a performance difference between the CM1 and CM4 channels in the case of CDD. Therefore, coding over higher number of subcarriers leads to significant performance gain of CDD. Analytical and simulation results agree to each other.

We have also evaluated the frame error rate (FER) of a half rate punctured convolutional code with constraint length 7 and the generator $g_0 = 133_8$, $g_1 = 165_8$, $g_2 = 171_8$ [15]. At FER of $10^{-3}$, CDD provides about 6 dB gain on the CM1 channel and about 3 dB gain on the CM4 channel. This shows that CDD provides a significant advantage in a practical coded system as well.

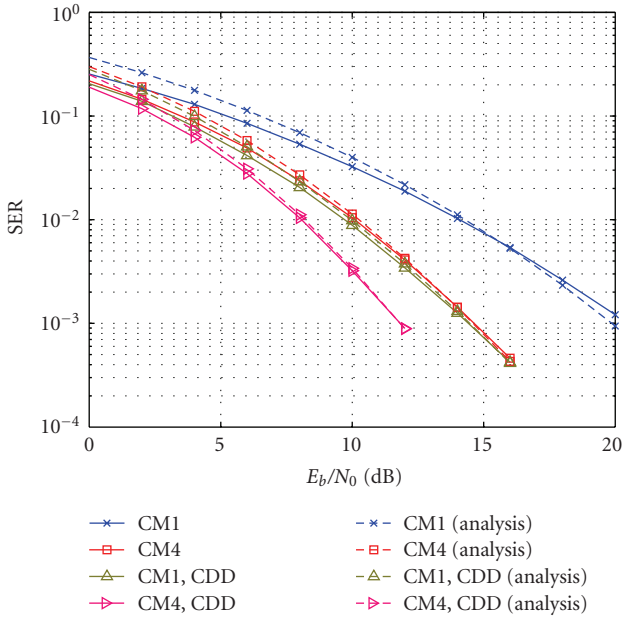


Figure 4: Symbol error rate of UWB-OFDM system. Jointly encoding across four subcarriers. CDD with two transmit antennas.

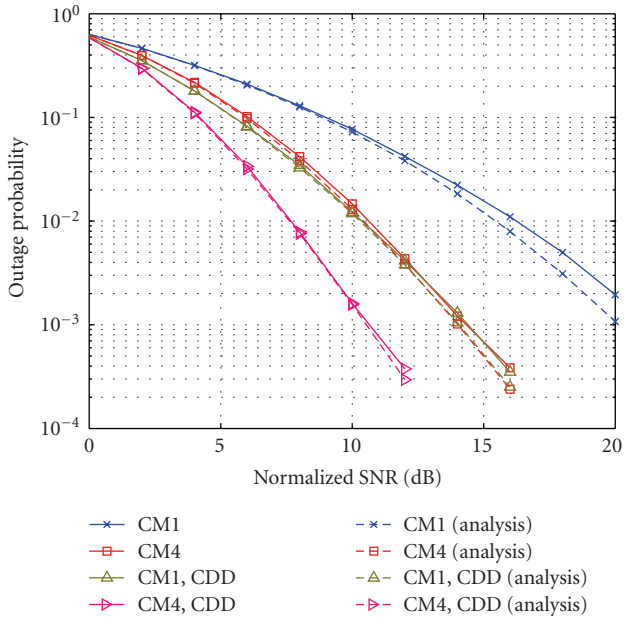


Figure 5: Outage probability of UWB-OFDM system. Jointly encoding across four subcarriers. CDD with two transmit antennas.

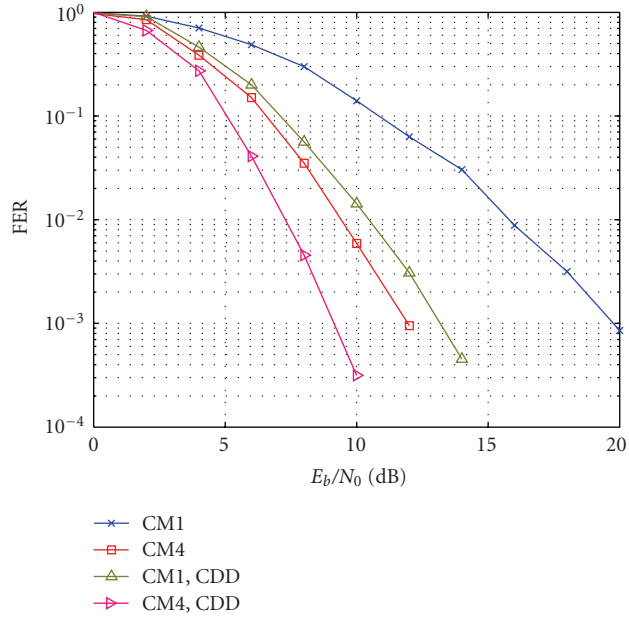


Figure 6: FER of a convolutional-coded UWB-OFDM system with/without cyclic delay diversity.

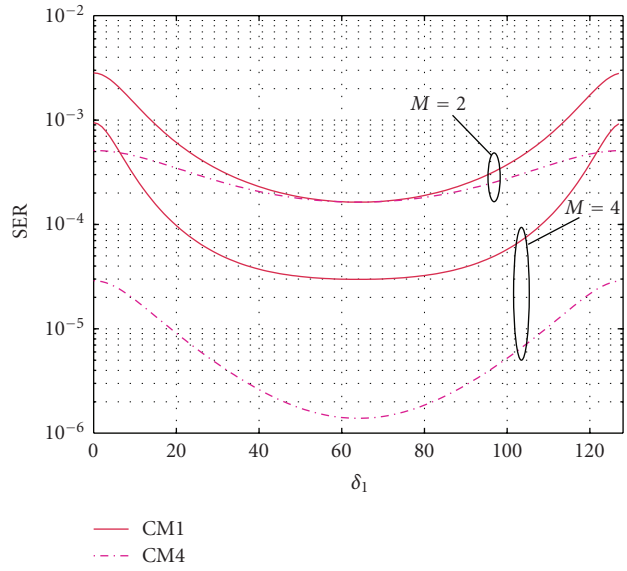


Figure 7: Symbol error rate as a function of delay time. CDD with two transmit antennas, $E_b/N_0 = 20$ dB, $\delta_0 = 0$.

## 6. DELAY TIME SELECTION OF CDD ON UWB-OFDM SYSTEM

Since the simulation and analytical results agree very well, one may perform an exhaustive search of the optimum delay times that minimize the SER from the union bound of (9) or the outage probability from (16). For example, using the same parameters as in Section 5 except the delay times, Figures 7 and 8 show the SER curves at $E_b/N_0 = 20$ dB and outage probability at normalized SNR of 20 dB as a function of delay time $\delta_1$, when $\delta_0 = 0$, respectively. From the figures, it can be deduced that the optimum $\delta_1$ that minimizes SER and outage probability occurs at $\delta_1 = 64$, that is, $N/2$ .

Although we can find the optimum delay times from exhaustive search for the case of two transmit antennas,the problem becomes very complex when the number of transmit antennas increases. The number of delay time choice in the exhaustive search is $N^{(N_t-1)}$ ($\delta_0$ can always be fixed at zero without loss of generality) which may be prohibitive even

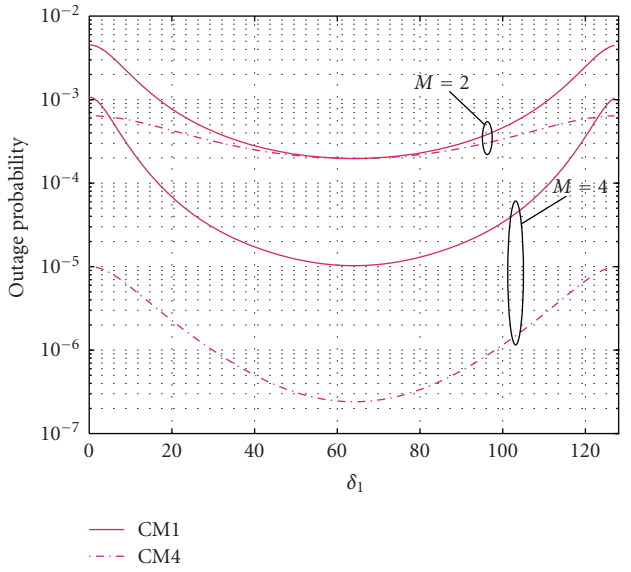


FIGURE 8: Outage probability as a function of delay time. CDD with two transmit antennas, normalized SNR = 20 dB, $\delta_0 = 0$.

when $N_t$ is not so high since $N$ is already high. Next, we try to find a closed form solution of the optimum delay time.

Although the case considered earlier shows that the optimum delay time for minimizing SER and outage probability occurs at the same value, it is not clear whether this is true in general. Now let us consider the objective of minimizing the SER computed from the union bound of (9). With the assumption of high $E_b/N_0$, (9) can be written as

$$P_e \approx \left(\prod_{n=1}^{\widehat{M}} \varphi_n\right)^{-1} \cdot \frac{1}{\pi} \int_0^{\pi/2} \prod_{n=1}^{M} \left(\frac{\rho \nu_n}{4N_t \sin^2\theta}\right)^{-1} d\theta, \tag{22}$$

where $\varphi_n$'s are nonzero eigenvalues of $\mathbf{R}_M^{\text{eff}}$, $\widehat{M}$ is the number of nonzero eigenvalues of $\mathbf{R}_M^{\text{eff}}$. Suppose $\mathbf{R}_M^{\text{eff}}$ has full rank (which is usually the case), (23) is equivalent to

$$P_e \approx \left(\det(\mathbf{R}_M^{\text{eff}})\right)^{-1} \cdot \frac{1}{\pi} \int_0^{\pi/2} \prod_{n=1}^{M} \left(\frac{\rho \nu_n}{4N_t \sin^2\theta}\right)^{-1} d\theta, \tag{23}$$

where $\det(\cdot)$ is a determinant. The second term of the product is independent of the delay times, so the optimum delay times can be found from

$$\{\delta_1, \delta_2, \ldots, \delta_{N_t-1}\}_{\text{opt}} = \underset{\{\delta_1,\delta_2,\ldots,\delta_{N_t-1}\}}{\arg\max} \det(\mathbf{R}_M^{\text{eff}}). \tag{24}$$

Next, the correlation matrix of the effective channel is rewritten as

$$\mathbf{R}_M^{\text{eff}} = \mathbf{R}_M \circ \boldsymbol{\Upsilon}, \tag{25}$$

where $\circ$ is a Hadamard (elementwise) product and

$$\boldsymbol{\Upsilon} = \begin{bmatrix} N_t & \sum_{n_t=0}^{N_t-1} e^{j(2\pi\delta_{n_t}/N)} & \cdots & \sum_{n_t=0}^{N_t-1} e^{j(2\pi\delta_{n_t}(M-1)/N)} \\ \ddot{Q} & N_t & \cdots & \sum_{n_t=0}^{N_t-1} e^{j(2\pi\delta_{n_t}(M-2)/N)} \\ \vdots & \vdots & \ddots & \vdots \\ Q & Q' & \cdots & N_t \end{bmatrix}, \tag{26}$$

where $Q$ denotes $\sum_{n_t=0}^{N_t-1} e^{-j(2\pi\delta_{n_t}(M-1)/N)}$, $Q'$ denotes $\sum_{n_t=0}^{N_t-1} e^{-j(2\pi\delta_{n_t}(M-2)/N)}$, and $\ddot{Q}$ denotes $\sum_{n_t=0}^{N_t-1} e^{-j(2\pi\delta_{n_t}/N)}$.

It is difficult to optimize (24) for a general case. However, for a special case when $N_t = M$, that is, when the number transmit antennas is equal to the number of symbols coded across subcarriers, the following result holds.

**Theorem 1.** *For $N_t = M$, the optimum delay times at high $E_b/N_0$ that minimize the SER are*

$$\delta_{n_t} = n_t \cdot \frac{N}{N_t}, \quad n_t = 0, 1, \ldots, N_t - 1. \tag{27}$$

*Proof.* Since $\mathbf{R}_M^{\text{eff}}$ is Hermitian and positive semidefinite by construction, applying Hadamard inequality [16], the determinant of an $M \times M$ matrix $\mathbf{R}_M^{\text{eff}}$ is maximized when the matrix is diagonal. The delay times chosen as in (6) cause the nondiagonal elements of $\boldsymbol{\Upsilon}$ to be zero (one can write each element in (26) using finite geometric series formula as in [6] to easily see this). So this choice makes $\boldsymbol{\Upsilon}$ and hence $\mathbf{R}_M^{\text{eff}}$ diagonal from (25), (26). □

Theorem 1 has shown that Witrisal et al. choice of delay times [4] is optimum in terms of minimizing the SER under high $E_b/N_0$, when $N_t = M$. When $N_t \neq M$, Witrisal et al. choice of delay times cannot make $\boldsymbol{\Upsilon}$ diagonal (in fact, it is not possible to make $\boldsymbol{\Upsilon}$ diagonal in such case). Other cases when $N_t \neq M$, other $E_b/N_0$ conditions and the optimum delay times that minimize the outage probability remain interesting problems.

## 7. CONCLUSION

This paper proposes CDD incorporated into UWB-OFDM systems. Symbol error rate and outage probability of CDD are derived analytically. It is shown that CDD improves the SER performance and reduces the outage probability significantly. The improvement is up to 6 dB gain over the CM1 channel with two transmit antennas. The simulation results validate all the analytical results. The issue of selecting the delay times is also addressed and a closed form solution is subsequently derived for a special case.

## ACKNOWLEDGMENTS

The authors would like to thank anonymous reviewers for their constructive and insightful comments. Part of this

paper is presented at International Conference on Information, Communications and Signal Processing (ICICS), 10–13 December 2007, Singapore.

## REFERENCES


[1] M. Z. Win and R. A. Scholtz, "Impulse radio: how it works," *IEEE Communications Letters*, vol. 2, no. 2, pp. 36–38, 1998.

[2] J. Balakrishnan, A. Batra, and A. Dabak, "A multi-band OFDM system for UWB communication," in *Proceedings of the IEEE Ultra Wideband Systems and Technologies Conference*, pp. 354–358, Dallas, Tex, USA, November 2003.

[3] WiMedia Alliance, http://www.wimedia.org/.

[4] K. Witrisal, Y.-H. Kim, R. Prasad, and L. P. Ligthart, "Antenna diversity for OFDM using cyclic delays," in *Proceedings of the 8th Symposium on Communication and Vehicular Technology*, pp. 13–17, Amsterdam, The Netherlands, October 2001.

[5] A. Dammann and S. Kaiser, "Standard conformable antenna diversity techniques for OFDM systems and its application to the DVB-T system," in *Proceedings of Conference IEEE Global Telecommunicatins Conference (GLOBECOM '01)*, vol. 5, pp. 3100–3105, San Antonio, Tex, USA, November 2001.

[6] A. Dammann, "On the influence of cyclic delay diversity and Doppler diversity on the channel characteristics in OFDM systems," in *Proceedings of IEEE International Conference on Communications (ICC '07)*, pp. 4179–4184, Glasgow, Scottland, June 2007.

[7] K.-B. Png, X. Peng, and F. Chin, "Performance studies of a multi-band OFDM system using a simplified LDPC code," in *Proceedings of the International Workshop on Ultra-Wideband Systems (IWUWBS '04)*, pp. 376–380, Kyoto, Japan, May 2004.

[8] T.-H. Tan and K.-C. Lin, "Performance of space-time block coded MB-OFDM UWB systems," in *Proceedings of the 4th Annual Communication Networks and Services Research Conference (CNSR '06)*, p. 5 pages, Moncton, New Brunswick, Canada, May 2006.

[9] N. Nyirongo, W. Q. Malik, and D. J. Edwards, "Concatenated RS-convolutional codes for ultrawideband multiband-OFDM," in *Proceedings of IEEE International Conference on Ultra-Wideband (ICUWB '06)*, pp. 137–142, Waltham, Mass, USA, September 2006.

[10] W. P. Siriwongpairat, W. Su, M. Olfat, and K. J. R. Liu, "Multiband-OFDM MIMO coding framework for UWB communication systems," *IEEE Transactions on Signal Processing*, vol. 54, no. 1, pp. 214–224, 2006.

[11] W. P. Siriwongpairat, W. Su, Z. Han, and K. J. R. Liu, "Employing cooperative diversity for performance enhancement in UWB communication systems," in *Proceedings of IEEE Wireless Communications and Networking (WCNC '06)*, vol. 4, pp. 1854–1859, Las Vegas, Nev, USA, April 2006.

[12] W. P. Siriwongpairat, W. Su, and K. J. R. Liu, "Performance characterization of multiband UWB communication systems using Poisson cluster arriving fading paths," *IEEE Journal on Selected Areas in Communications*, vol. 24, no. 4, pp. 745–751, 2006.

[13] J. Foerster, et al., "Channel modeling sub-committee report final," IEEE 802.15-02/490, 2003.

[14] G. Bauch and J. S. Malik, "Cyclic delay diversity with bit-interleaved coded modulation in orthogonal frequency division multiple access," *IEEE Transactions on Wireless Communications*, vol. 5, no. 8, pp. 2092–2100, 2006.

[15] ECMA International, "High rate ultra wideband PHY and MAC standard," ECMA-368, 1st Edition, December 2005.

[16] R. A. Horn and C. R. Johnson, *Matrix Analysis*, Cambridge University Press, Cambridge, UK, 1985.